FINAL REPORT

Variability of Rossby Wave Breaking and its Impacts on the Large-scale Circulation and Extreme Weather: Implications for S2S Prediction and Predictability

Lead PI: Zhuo Wang, Professor
Department of Atmospheric Sciences
University of Illinois at Urbana-Champaign
105 South Gregory St., Urbana IL 61801
Phone: (217) 244-4270, Email: zhuowang@illinois.edu

Institutional representative: Walter K. Knorr, Comptroller
1901 S. First Street, Suite A, Champaign, IL 61820-7406
Phone: (217) 333-2187, Fax: (217) 239-6830, E-mail: osp@illinois.edu

Co-PI: Melinda Peng
Naval Research Laboratory (NRL)
Marine Meteorology Division, Atmospheric Dynamics and Prediction Branch

Co-PI: Stan Benjamin
NOAA Earth System Research Laboratory (ESRL), Global Systems Division

Reporting Period: 07/01/2016 - 06/30/2020
Grant #: NA16OAR4310080

1. Main goals of the project

Rossby wave breaking (RWB) is characterized by large-scale, irreversible overturning of potential vorticity (PV) on isentropic surfaces. The eddy-mean interaction involved in RWB is an important process for the maintenance and variability of the midlatitude jet, and the mixing associated with RWB plays an important role in moisture and momentum transport between the tropics and extratropics. RWB is also related to extreme weathers, such as blocking and atmospheric rivers.

The goal of the project is to better understand the variability and predictability of RWB on the subseasonal to seasonal (S2S) time scales and to improve the prediction skill of RWB-related extreme weather. In particular, we have

- examined the variability and impacts of Rossby wave breaking (RWB) on S2S time scales using reanalysis and satellite data
- investigated the implications of the findings for the S2S prediction and predictability of extreme weather.

Results are summarized in section 2, under the above two subtopics.

2. Results and accomplishments

Variability and Impacts of Rossby Wave Breaking

2.1 Characteristics and Impacts of Extratropical Rossby Wave Breaking during the Atlantic Hurricane Season (Zhang et al. 2017)

We investigated the characteristics of extratropical Rossby wave breaking (RWB) during the Atlantic hurricane season and its impacts on Atlantic tropical cyclone (TC) activity. It was found that RWB perturbs the wind and moisture fields throughout the troposphere in the vicinity of a breaking wave (Fig. 1). When RWB occurs more frequently over the North Atlantic, the Atlantic main development region (MDR) is subject to stronger vertical wind shear and reduced tropospheric moisture; the basin-wide TC counts are reduced, and TCs are generally less intense, have a shorter lifetime, and are less likely to make landfalls (Fig. 2). A significant negative correlation was found between Atlantic TC activity and RWB occurrence during 1979– 2013. The correlation is comparable to that with the MDR SST index and stronger than that with the Niño-3.4 index.

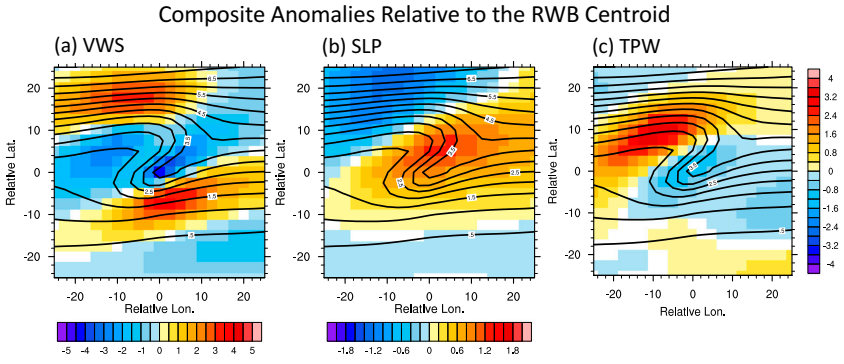

Fig. 1 Composites of anomalies in (a) vertical wind shear, (b) SLP and (c) total precipitable water relative to the RWB centroid (signals below the 95% confidence level are not shown).

Further analyses suggest that the variability of RWB occurrence in the western Atlantic is largely independent of that in the eastern Atlantic. The RWB occurrence in the western basin is more closely tied to the environmental variability of the tropical North Atlantic and is more likely to hinder TC intensification or reduce the TC lifetime because of its proximity to the central portion of TC tracks. Consequently, the basin-wide TC counts and the accumulated cyclone energy have a strong correlation with western-basin RWB occurrence but only a moderate correlation with eastern-basin RWB occurrence. The results highlight the extratropical impacts on Atlantic TC activity and regional climate via RWB and provide new insights into the variability and predictability of TC activity.

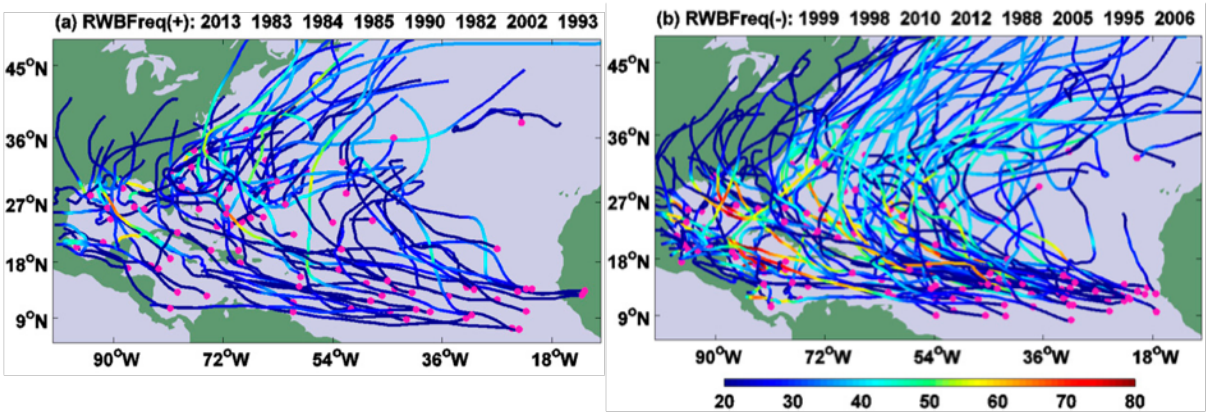

Fig. 2 Composite of TC tracks of (a) RWBFreq+ group and (b) RWBFreq- group. The pink dots highlight the locations of TC genesis, and the coloring represents the wind speed (m s21) of TCs. The composite members of each group are denoted in the subplot titles.

2.2 North Atlantic Extratropical Rossby Wave Breaking: Wave Life Cycle and Role of Diabatic Heating (Zhang and Wang 2018)

Zhang and Wang (2018) investigated the life cycle of anticyclonic Rossby wave breaking during the extended warm season (July–October) over the North Atlantic basin. It was found that upper-tropospheric breaking waves are coupled with lower-level perturbations and can be traced back to a wave train that extends from the North Pacific. The overturning of potential vorticity (PV) contours during wave breaking is associated with the rapid development of an upper-level ridge, which occurs along the east coast of North America and over a warm and moist airstream. The ridge development is investigated using the PV budget analysis and trajectory analysis. The PV budget analysis suggests that the horizontal advection of PV by the perturbed flow dictates the movement and the later decay of the ridge. The ridge amplification, opposed by the horizontal advection of PV, is driven by the vertical advection and the diabatic production of PV, both of which are connected to diabatic heating (Fig. 3). The vital role of diabatic heating in the ridge amplification is corroborated by the trajectory analysis. The analysis suggests that diabatic heating reduces the static stability near the tropopause and contributes to the ridge-related negative PV anomalies. The role of diabatic heating in anticyclonic and cyclonic wave breaking in other regions is also discussed. The findings suggest that moist diabatic processes, which were often excluded from the earlier studies of wave breaking, are crucial for Rossby wave breaking during the warm season. The updated understanding of wave breaking may benefit weather forecasting and climate predictions.

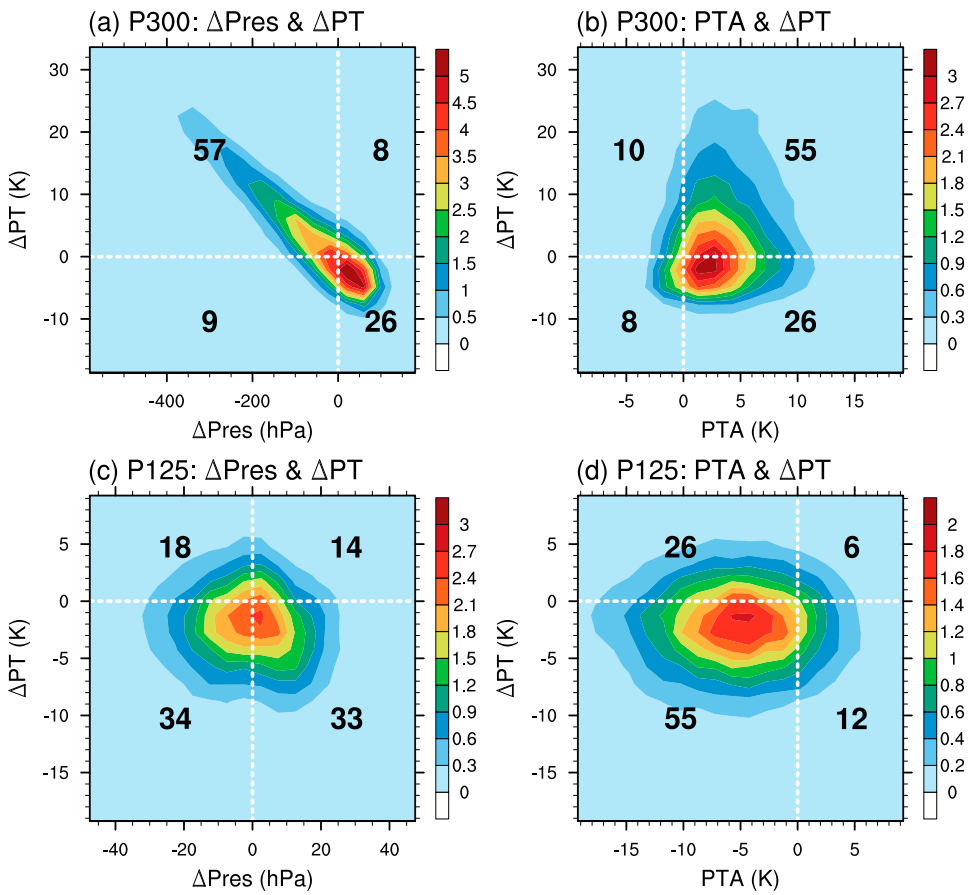

Fig. 3 Diabatic heating experienced by the ridge-associated air parcels from T 5 296 to T 5 0 h. (a),(c) PDFs of the potential temperature changes (DPT) and the vertical displacement (DPres) experienced by air parcels in the 300- and 125-hPa groups (see the text for more details). (b),(d) PDFs of the potential temperature changes and the potential temperature anomalies (PTA) at T 5 0 h. All the changes are calculated as the state at T 5 0 h minus the state at T 5 296 h, so the positive values along the vertical axes of (a)–(d) and the negative values along the horizontal axes of (a),(c) correspond to heating and ascending, respectively. The white dashed lines separate the domains into four quadrants, and the sums of the PDFs in each quadrant are shown at the corresponding quadrant center.

2.3 North Atlantic Rossby Wave Breaking during the Hurricane Season: Association with Tropical and Extratropical Variability (Zhang and Wang 2019)

Our previous studies have shown that anticyclonic RWB events strongly influence Atlantic TC activity on the intraseasonal-to-seasonal scale (Zhang et al. 2016; 2017; Papin 2017; Li et al. 2018). This study focuses on the events over the western subtropical basin (RWBw), which have relatively strong impacts on Atlantic TC activity (Zhang et al. 2017), and explores what may drive the variations of RWB. Our findings suggest that the variations of the RWBw events are tied to both tropical and extratropical variations on the weather-climate continuum.

Zhang and Wang (2019) explored the connection of Rossby wave breaking (RWB) with tropical and extratropical variability during the Atlantic hurricane season. The exploration emphasizes

subtropical anticyclonic RWB events over the western North Atlantic, which strongly affect tropical cyclone (TC) activity. The first part of the study investigates the link between RWB and tropical sea surface temperature (SST) variability. Tropical SST variability affects tropical precipitation and modulates the large-scale atmospheric circulation over the subtropical Atlantic, which influences the behaviors of Rossby waves and the frequency of RWB occurrence. Meanwhile, RWB regulates surface heat fluxes and helps to sustain SST anomalies in the western North Atlantic. The second part of the study explores the connections between RWB and extratropical atmosphere variability by leveraging weather regime analysis. The weather regimes over the North Atlantic are closely associated with RWB over the eastern North Atlantic and western Europe, but show weak associations with RWB over the western North Atlantic. Instead, RWB over the western basin is closely related to the weather regimes in the North Pacific–North America sector (Fig. 4). The finding helps clarify why the correlation between the Atlantic TC activity and the summertime North Atlantic Oscillation is tenuous. The relations between the extratropical weather regimes and tropical climate modes are also discussed. The findings suggest that both tropical and extratropical variability are important for understanding variations of RWB events and their impacts on Atlantic TC activity.

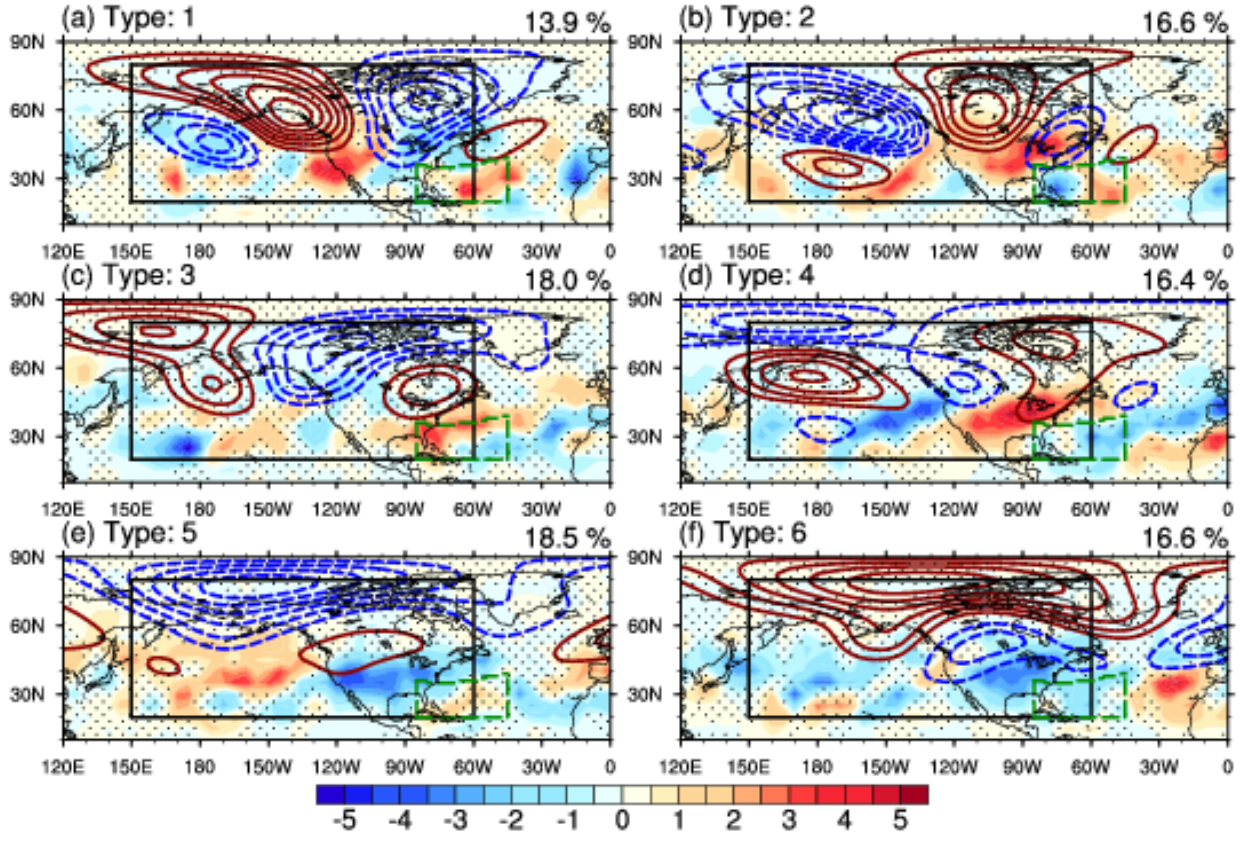

Fig. 4 Weather regimes over the North Pacific and North America (150°E–60°W, 20°N–80°N). The contours show the anomalies of 200-hPa geopotential height, and the color shading shows the variations of RWB occurrences on the 350-K isentropic surface. The variations of RWB occurrences lag the weather regimes by 5 days.

2.4 Predictability of North Atlantic Tropical Cyclogenesis in the Flow Regimes Related to RWB (Wang et al. 2018)

The practical predictability of tropical cyclogenesis over the North Atlantic was examined in different synoptic flow regimes using the NCEP GEFS reforecasts. Flow regimes were identified objectively by five tropical cyclogenesis pathways that are categorized based on the upper-level forcing and low-level baroclinicity of the environmental atmospheric state (McTaggart-Cowan et al. 2013). Among them, the non-baroclinic (NBC) and low-level baroclinic (LBC) pathways have negligible upper-level forcing and can be regarded as purely tropical pathways; trough-induced, weak tropical transition (TT; Davis and Bosart 2004), and strong TT pathways are subject to strong upper-level forcing that are often associated with RWB (Bentley et al. 2017), and can be regarded as hybrid or extratropical pathways. The analysis of the GEFS reforecasts suggests that the extratropical/hybrid pathways have lower predictability than the tropical pathways (see examples in Fig. 5), and the RMSEs of vertical wind shear and 700-hPa relative humidity help to explain the different predictive skills for different pathways. The low predictability of tropical transition pathways is consistent with the general perception that the extratropical atmosphere is less predictable than the tropical atmosphere for forecast lead time beyond a few days (Davis et al. 2016).

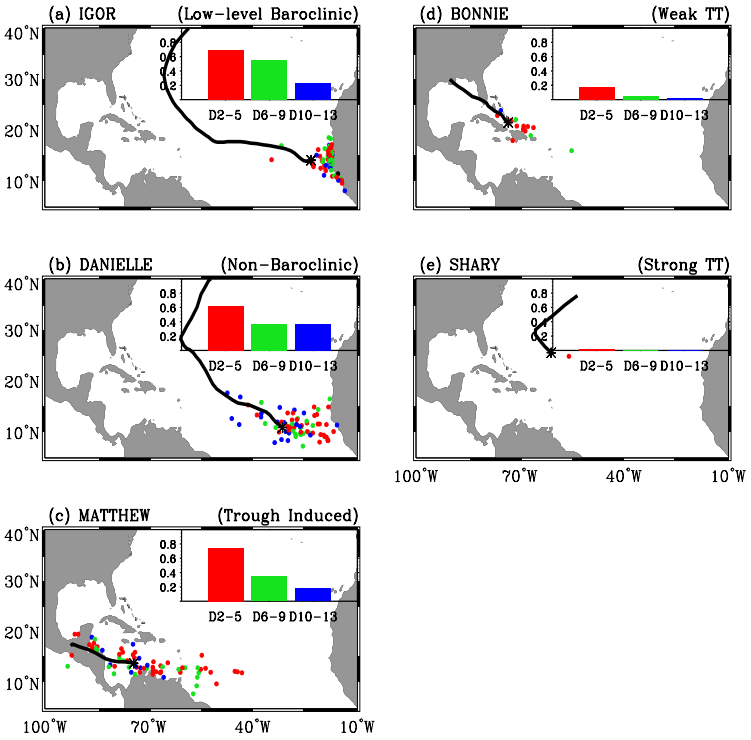

Fig. 5 Illustrative cases for each genesis pathway in 2010. Black curves represent the observed tracks, and dots of different colors represent forecast genesis locations at different lead times. The insets show the ensemble hit rates at different lead times.

Previous studies have reported that the predictive skill of a model in tropical cyclogenesis varies from region to region and from month to month. Large spatial variations of the hit rate were also found in this study: the MDR region has a higher hit rate than the Gulf of Mexico or the subtropical Atlantic (the false alarm ratio is similar and very large in all the regions). These spatial variations can be largely explained by the different relative contributions of the pathways in different regions. The relatively frequent occurrence of TT pathways over the Gulf of Mexico and the subtropical Atlantic contributes to the lower genesis predictability in these regions. In addition, the purely tropical pathways (NBC and LBC) occur more frequently in August and September, and this contributes to a relatively high hit rate in the peak hurricane season compared to the early and late seasons. This suggests that storms developing near the southeast coast of North America, which are more likely subject to strong extratropical influences, may pose a particular challenge for operational forecasts and emergency management. Knowledge of the predictability of such coastal storms can assist decision-making by providing useful estimates of predictive skill before forecast validation becomes available.

2.5 Subseasonal Variability of Rossby Wave Breaking and Impacts on Atlantic Tropical Cyclones (Li et al. 2018)

The subseasonal variability of anticyclonic Rossby wave breaking (AWB) and its impacts on the large-scale atmospheric condition and tropical cyclones were investigated during the Atlantic warm season (July-October) from 1985 to 2012 (28 years). The analyses show that AWB modulates both the upper- and lower-tropospheric circulations, and is associated with the variability of vertical wind shear, tropospheric humidity, and precipitation on the subseasonal timescale. The atmospheric circulation anomalies are related to a Rossby wave train spanning from North America to the North Atlantic. Statistically significant anomalies are found within 8 days (± 4 days) of an AWB activity peak, which results in suppressed TC activity over the Atlantic central and western main development region (MDR) and the subtropical western North Atlantic, especially along the climatological tropical upper tropospheric trough (TUTT) region.

However, the linear correlations between the weekly AWB index and weekly TC indices within a season vary strongly from year to year, and significant negative correlations exist only in some years. In particular, the negative AWB-TC correlation is more pronounced during the years of enhanced Madden-Julian oscillation (MJO) activity and tends to be stronger in the El Niño and neutral years than in the La Niña years, but the AMM has little impact. Composite analysis shows that the subseasonal variation of AWB is closely tied to the MJO and the MJO-related teleconnections, showing an eastward progression along with the MJO. Although it is challenging to separate the impact of AWB from that of the MJO due to the possible interaction between AWB and the MJO, our analyses indicate that the correlation between the MJO and TCs tends to be stronger during years of enhanced AWB activity, and suggest the possibility that active AWB may help to enhance the MJO signals and the subseasonal MJO-TC correlation.

The impacts of AWB on the Atlantic TC prediction were investigated using the NCEP Global Ensemble Forecasting System (GEFS) reforecasts. The GEFS exhibits a lower hit rate of TC genesis than long-term mean hit rate during the active AWB episodes (not shown), which is consistent with the lower predictability of the ambient vertical wind shear, tropospheric humidity, and low-level relative vorticity (Fig. 6). The GEFS is also less skillful in capturing the active/inactive TC periods within a season during the years of enhanced AWB activity, which suggests that active AWB tends to reduce TC predictability on the subseasonal timescale.

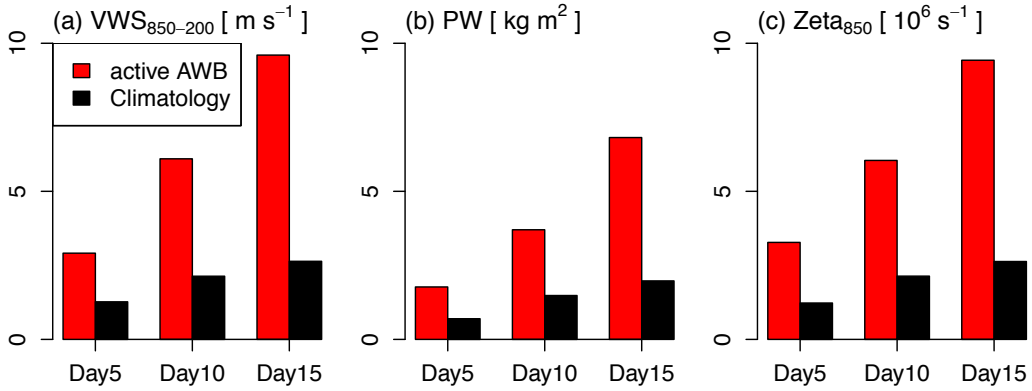

Fig. 6 Ensemble spread of the ambient (a) vertical wind shear, (b) the precipitable water (PW), and (c) 850-hdPeeap relative vorticity for all the Atlantic TCs (black; 316 cases) and for the AWB-related TCs (red; 74 cases) during 1985-2012 JASO in the GEFS reforecasts.

This study focuses on the impacts of RWB on TCs over the Atlantic. Recent studies suggested that recurving TCs may induce amplified Rossby wavetrains and RWB downstream (e.g., Riemer and Jones 2014; Archambault et al. 2015). An integrated, global picture of the complex interaction among the MJO, TCs, and RWB will help to better understand the variability and predictability of tropical weather and climate systems on the subseasonal timescale.

2.6 Relative Impacts of Local and Remote Forcing on Tropical Cyclone Frequency in Numerical Model Simulations (Chang and Wang 2018)

Three groups of numerical experiments are carried out to investigate the importance of local and remote forcing on TC frequency. The first two groups of experiments focus on the regional simulations of Atlantic TCs, and the third group examines the TC activity in the northern tropics using a tropical channel configuration. The first group of experiments reproduce the active hurricane season in 2005 and the inactive season in 2013 when driven by the observed surface temperature and LBCs from the corresponding years (Fig. 7). The mixed simulations, with surface temperature from 2005 and LBCs from 2013, resemble the 2013 simulations, which implies the strong influence of remote forcing on Atlantic TCs (Fig. 7). The hurricane seasons from 2000-2016 are simulated in the second group of experiments. The interannual variability of Atlantic TC frequency is skillfully simulated by the control run as indicated by the correlation between the observed and simulated TC counts (r=0.63). The correlation is reduced when the LBCs are set to 2013 (r=0.22) or the surface temperature is set to 2005 (r=0.42). This suggests that the remote and local impacts both modulate Atlantic TC frequency, and the larger reduction of correlation in Exp2-LBC13 suggests that the remote forcing may have stronger impacts on Atlantic TCs than the local SST. Pattern correlation analysis further suggests that the tropospheric variability is strongly modulated by remote forcing. The tropical channel experiments in Group 3 fail to skillfully simulate the interannual variability of the total TC counts in the northern tropics. However, the strong correlation of TC counts between Exp3-CTRL and Exp3-LBC13, which have the same SST forcing but different LBCs, suggests that tropical SST plays a dominant role in modulating the total TC activity over the northern tropics, in contrast to the Atlantic basin.

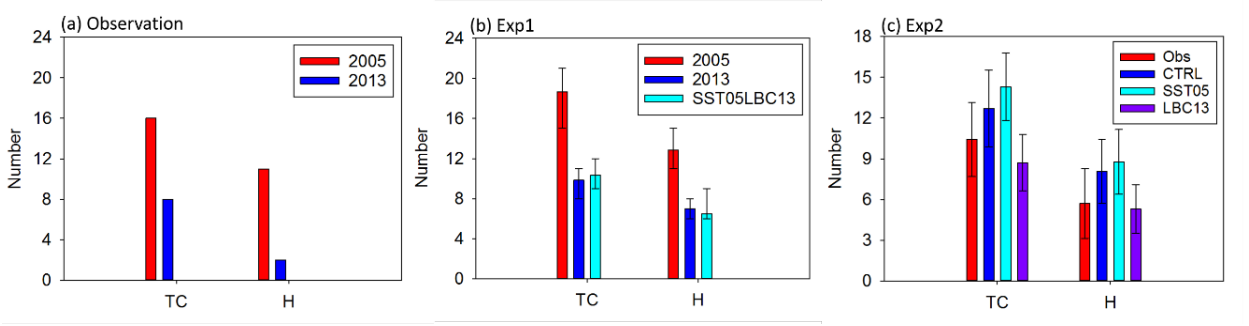

Fig. 7 Tropical cyclone counts and hurricane counts from (a) the IBTrACS, (b) Experiment Group 1 and (c) Experiment Group 2. The bars in (b) are the ensemble mean with whiskers showing the ensemble range; the bars in (c) are the average over 2000-2016 with whiskers indicating the interannual standard deviation. (from Chang and Wang 2018)

The experiments suggest that the remote forcing plays an important role in modulating Atlantic TC activity and that the influence may even exceed that of local SST in some years. However, the results should not be interpreted as that the influence of tropical SST on Atlantic TC activity is not important. It is worth noting that 2013 is characterized by very active RWB over the North Atlantic and that such strong extratropical influence does not exist in every year.

Some results in this study may be sensitive to the model configuration. In particular, it is conceivable that LBCs may have a weaker control on regional model simulations if the model domain is larger. This helps to explain the difference in the local vs. remote control on TC activity between the Atlantic basin and the northern tropics, but we suspect that the differences are also tied to the forcing mechanisms of TC variability in different basins. For example, TC variability tends to be out-of-phase between the North Atlantic and the East Pacific [e.g., Wang and Lee, 2009; Zhang et al., 2015]. Such TC variations are partly cancelled when the northern tropics is considered as a whole, so the regional TC variability may not be closely related to the global TC variability. In addition, TCs are strongly modulated by the ENSO in the East Pacific [e.g., Jin et al., 2014; Zhang and Wang, 2015] and are closely tied to the monsoon activity over the western North Pacific [e.g., Ritchie and Holland, 1999]. Extratropical influence may thus be relatively weak in these basins. The sensitivity of Atlantic TCs to extratropical processes may help to explain the uncertainties in the projections of future Atlantic TC activity.

2.7 Linking Atmospheric River Hydrological Impacts on the U.S. West Coast to Rossby Wave Breaking (Hu et al. 2017)

Atmospheric rivers (ARs) have significant hydrometeorological impacts on the U.S. West Coast. We examined the connection between the characteristics of large-scale RWB over the eastern North Pacific and the regional-scale hydrological impacts associated with landfalling ARs on the U.S. West Coast (36°–49°N). ARs associated with RWB account for two-thirds of the landfalling AR events and >70% of total AR-precipitation in the winter season (Fig. 8 left). The two regimes of RWB—anticyclonic wave breaking (AWB) and cyclonic wave breaking (CWB)—are associated with different directions of the vertically integrated water vapor transport (IVT) (Fig. 8 right). AWB-ARs impinge in a more westerly direction on the coast whereas CWB-ARs impinge in a more southwesterly direction.

Most of the landfalling ARs along the northwestern coast of the United States (Washington and

Oregon) are AWB-ARs. Because of their westerly impinging angles when compared to CWB-ARs, AWB- ARs arrive more orthogonally to the western Cascades and more efficiently transform water vapor into precipitation through orographic lift than CWB-ARs (Fig. 8). Consequently, AWB-ARs are associated with the most extreme streamflows in the region.

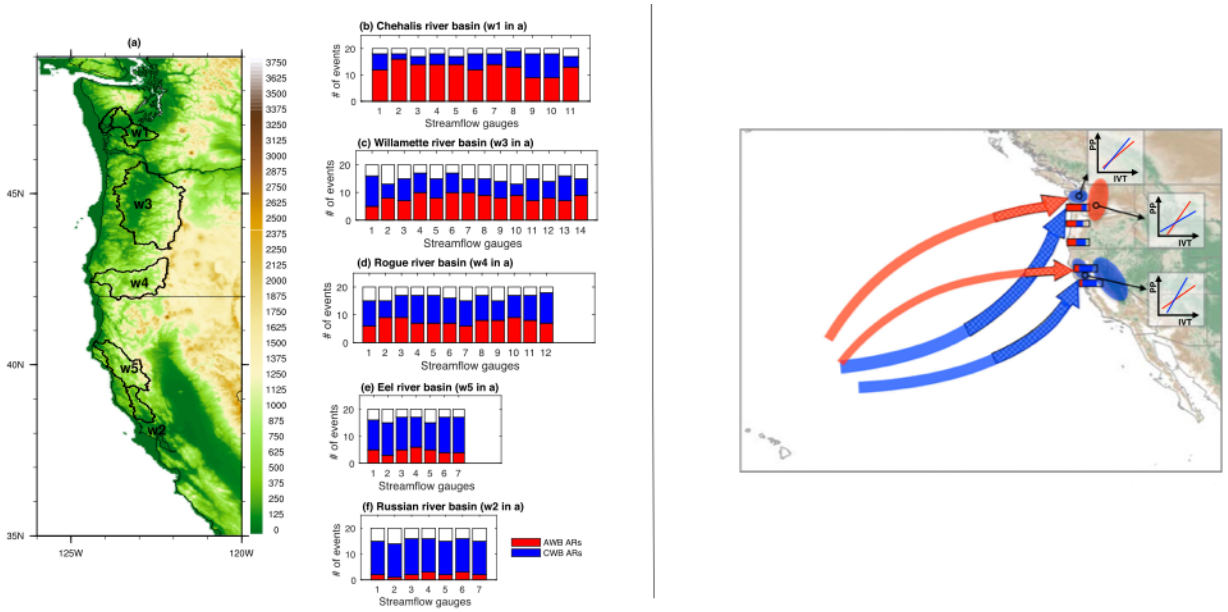

Fig. 8 ***(Left)*** *(a) The five river basins along the West Coast, and the number of top 20 streamflow events due to AWB- (red bars) and CWB- (blue bars) ARs.* ***(Right)*** *Schematic showing the averaged maximum IVT axes of AWB- (red) and CWB-ARs (blue) impinging toward the northern and southern U.S. coasts (impinging angles indicated by the thick arrows). The thicknesses of the curves suggest the magnitude of the averaged IVT magnitude. Red (blue) shaded ellipses suggest where positive precipitation anomaly is resulted from AWB-ARs (CWB-ARs). The compositions of the extreme streamflow events due to AWB-ARs (red bars) and CWB-ARs (blue bars) are shown by the horizontally aligned bars over the general basin locations. The efficiencies of AWB-ARs (CWB-ARs) in converting IVT to precipitation (or PP), obtained from the locations of the black circles, are shown by the slopes of the red (blue) lines in the x–y plots.*

Along the southwest coast of the United States (California), the southwesterly impinging angles of CWB- ARs are more orthogonal to the local topography. Furthermore, the southwest coast CWB-ARs have more intense IVT. Consequently, CWB-ARs are associated with the most intense precipitation. As a result, most of the extreme streamflows in southwest coastal basins are associated with CWB-ARs. In summary, depending on the associated RWB type, ARs impinge on the local topography at a different angle and have a different spatial signature of precipitation and streamflow.

2.8 Intraseasonal Tropical Cyclogenesis Prediction in a Global Coupled Model System (Jiang et al. 2018)

Motivated by increasing demand in the community for intraseasonal predictions of weather extremes, predictive skill of tropical cyclogenesis is investigated based on a global coupled model system. Limited intraseasonal cyclogenesis prediction skill with a high false alarm rate is found when averaged over about 600 tropical cyclones (TCs) over global oceans from 2003 to 2013,

particularly over the North Atlantic (NA). Relatively skillful genesis predictions with more than 1-week lead time are only evident for about 10% of the total TCs. Further analyses suggest that TCs with relatively higher genesis skill are closely associated with the Madden– Julian oscillation (MJO) and tropical synoptic waves, with their geneses strongly phase-locked to the convectively active region of the MJO and low-level cyclonic vorticity associated with synoptic-scale waves (Fig. 9). Moreover, higher cyclogenesis prediction skill is found for TCs that formed during the enhanced periods of strong MJO episodes than those during weak or suppressed MJO periods (Fig. 9). All these results confirm the critical role of the MJO and tropical synoptic waves for intraseasonal prediction of TC activity. Tropical cyclogenesis prediction skill in this coupled model is found to be closely associated with model predictability of several large-scale dynamical and thermodynamical fields. Particularly over the North Atlantic, higher predictability of low-level relative vorticity, midlevel humidity, and vertical zonal wind shear is evident along a tropical belt from the West Africa coast to the Caribbean Sea, in accord with more predictable cyclogenesis over this region. Over the extratropical North Atlantic, large-scale variables exhibit less predictability due to influences of extratropical systems, leading to poor cyclogenesis predictive skill.

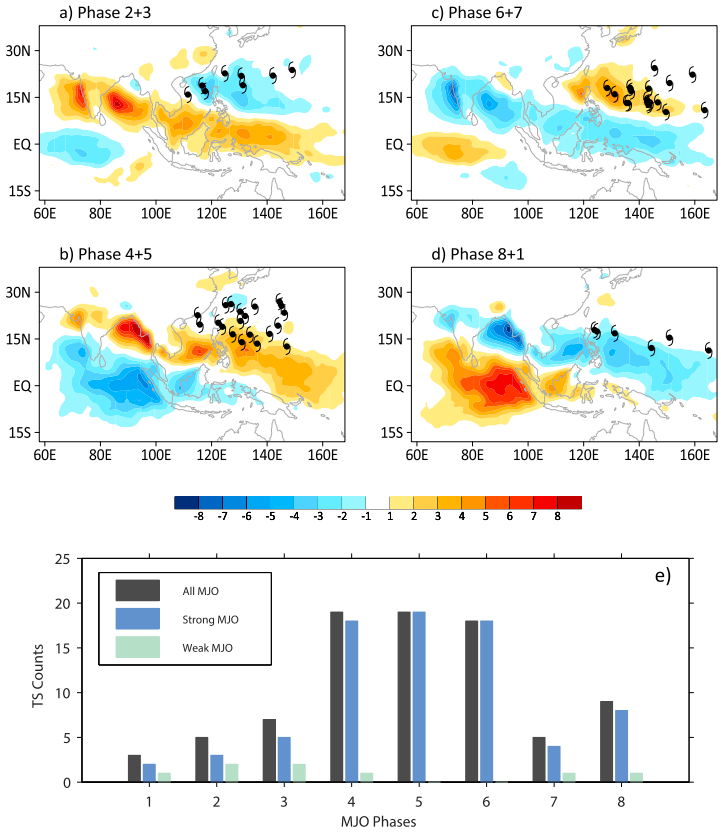

Fig. 9 (a)–(d) Genesis of the more predictable TCs over the WP from 2003 to 2013 during different local MJO phases. Shading represents the observed anomalous rainfall pattern (mm/day) during each MJO phase. (e) Counts of more predictable TC genesis over the West Pacific as a function of MJO phases under both strong and weak MJO periods. MJO phases shown here are defined based on PCs of the two leading EEOF modes of 10–70-day filtered rainfall over the West Pacific for summers of 2003–13.

2.9 Summertime Stationary Eddies Integrate Tropical and Extratropical Impacts on TC Activity (Wang et al. 2020)

Tropical cyclones (TC) are one of the most severe storm systems on the planet of earth and can cause significant life loss and property damage in coastal areas. A better understanding of the variability mechanisms of TC activity will help improve the TC prediction skill on the seasonal to interannual time scales. Early studies primarily focused on tropical processes, while some recent studies suggested the impacts of extratropical processes on TC activity. We demonstrated that the summertime stationary eddies, including the tropical upper-tropospheric troughs (TUTTs), integrate tropical and extratropical impacts on TC activity and provide a global perspective on the variability of TC activity over the North Pacific and North Atlantic.

To quantify the relationship between TUTTs and TC activity, a TUTT index is defined based on the equatorward extension of the upper-level westerly flow over a subtropical ocean. Two TUTT indices are derived, one representing the North Pacific TUTT (TUTT_Pac) and the other the North Atlantic TUTT (TUTT_Atl). Composite analysis revealed that the variability of a TUTT is associated with significant anomalies in wind shear, tropospheric humidity, and RWB occurrence in both the North Atlantic and North Pacific. RWB frequency increases significantly when the TUTT is strong in that basin (not shown), which transports cold and dry extratropical air equatorward and increases the thickness gradient and tropospheric dryness to its south. The extensive upper-level westerlies associated with a deeper TUTT facilitate equatorward Rossby wave propagation and breaking. Meanwhile, transient eddy feedback likely helps maintain or amplify a TUTT. The seasonal variability of TUTTs thus reflects the cumulative impacts of RWB beyond the synoptic time scale.

Consistent with the changes in the large-scale circulation anomalies, TC track density function (TDF) is reduced when the TUTT is strong in that basin (Fig. 10). Significant negative correlations are found between a TUTT index and the basin-wide TC frequency (TCF), hurricane frequency (HURR) and accumulative cyclone energy (ACE) in the North Atlantic, western North Pacific and eastern North Pacific (Table 1). In fact, the seasonal correlations of the TC indices with the TUTT index in that basin are much stronger than the corresponding correlations with the Nino3.4.

Another interesting feature in the TDF composites is the out-of-phase TC variability between the Atlantic and Pacific basins, which is consistent with the seesaw tendency of the Pacific and Atlantic TUTTs. The anticorrelation between TUTT_Pac and TUTT_Atl can be explained by the PV impermeability theorem. An important implication is the out-of-phase relationship of TC activities between the Atlantic and Pacific basins [*r=-0.47, -0.44 and -0.42* for TCF, HURR and ACE between the North Pacific (the sum of the western Pacific and the eastern Pacific) and North Atlantic, respectively]. Since the North Pacific and North Atlantic together account for more than 60% of the global TC frequency, the anticorrelation between the two basins makes the global TC activity less variable. This TC anticorrelation has been examined in some previous studies and attributed to the modulation by the Walker circulation. TUTTs offer an additional mechanism for this inter-basin relationship.

TUTTs are part of the summertime stationary eddies. Using the EOF analysis, we extracted the leading mode of the non-zonal 200-hPa streamfunction, which is significantly correlated to TUTT_Pac and TUTT_Atl. Correlation analysis reveal significant SST and precipitation signals

in various regions in the tropics and subtropics. Although EOF1 is significantly correlated to the Nino3.4, partial correlation analysis suggests that the ENSO is just one of the factors modulating the summertime stationary eddies and TUTTs. After the linear impacts of the ENSO are removed, the strong correlations between TUTTs and TC activity still exist.

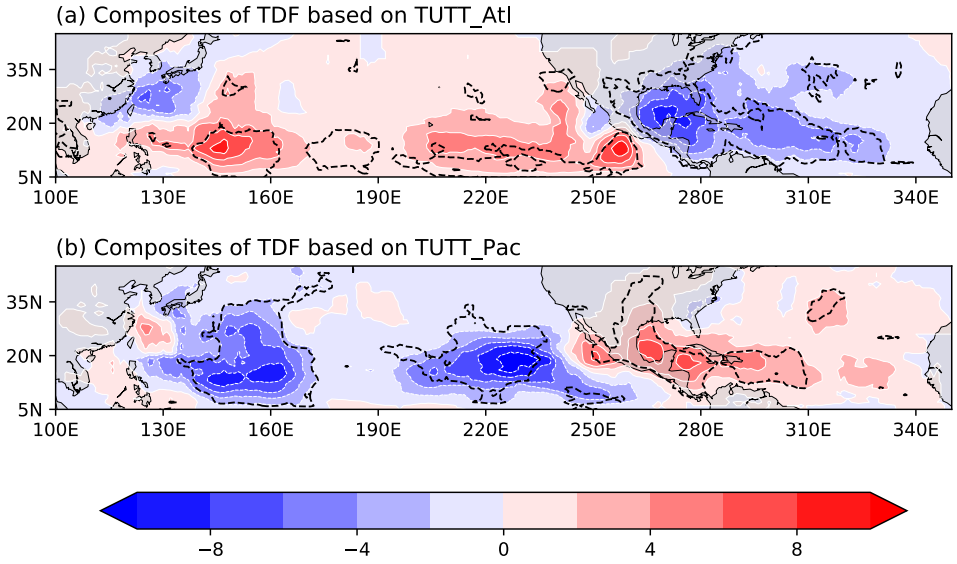

Fig. 10 Composites of tropical cyclone track density function (units: number of TCs per month within a 10°×10° grid box) based on (a) TUTT_Atl and (b) TUTT_Pac. Black contours depict the anomalies exceeding the 95% confidence level.

Table 1 Correlation coefficients between different climate indices and the TC activity indices over three basins during JASO 1979-2018. RWB is the RWB frequency between 10-85°W, south of the jet axis and north of 20°N (see Zhang et al. 2017 for more details).

Corr.	TCF	HURR	ACE
	Atlantic TC Indices		
TUTT_Atl	-0.73	-0.76	-0.75
MDR	0.59	0.56	0.55
Nino3.4	-0.34	-0.38	-0.32
RWB	-0.46	-0.56	-0.68
EOF1	0.54	0.58	0.50
	East Pacific TC Indices		
TUTT_Pac	-0.60	-0.58	-0.63
Nino3.4	0.39	0.28	0.46
EOF1	-0.60	-0.50	-0.58
	West Pacific TC Indices		
TUTT_Pac	-0.45	-0.53	-0.61
Nino3.4	0.01	0.18	0.56
EOF1	-0.30	-0.46	-0.69

The global nature of stationary eddies highlights the global nature of the TC variability problem and provides a non-tropical pathway for a remote forcing to affect TC activity. This global perspective is consistent with some recent findings on the link between the Indian summer monsoon and Atlantic TC tracks and the link between Central Pacific SST and Atlantic RWB occurrence. Overall, we advocate a global perspective to understand the variability and predictability of TC activity. This view may also help understand the projection of TC activity in future climate.

2.10 Multiyear Hybrid Prediction of Atlantic Tropical Cyclone Activity and the Predictability Sources (Chang et al. 2020)

We develop a skillful statistical-dynamical model for multi-year prediction of Atlantic TC activity. The dynamical predictions of SST are based on the Community Earth System Model decadal prediction dataset (CESM-DP; Yeager et al. 2018). The statistical component of the hybrid model is a Poisson model that takes the Atlantic MDR and SPG SST indices as predictors. The hybrid prediction is evaluated against the HURDAT2 data using the leave-five years-out method, and the hybrid model exhibits significant skills for the basin-wide TC frequency, ACE, landfalling TC frequency, as well as hurricane and major hurricane days.

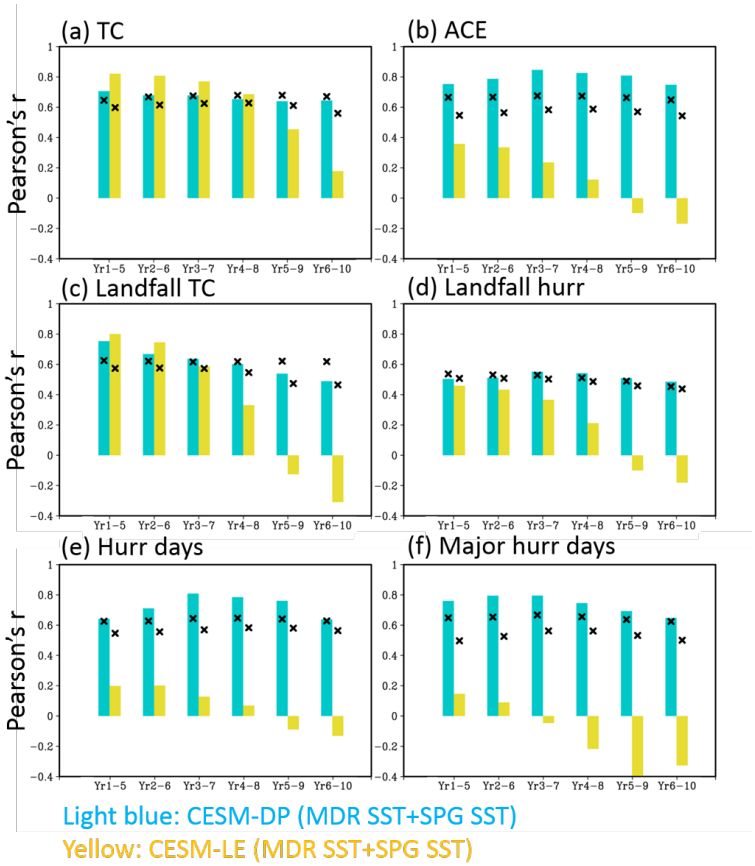

Fig. 11 Prediction skills of various TC indices at different forecast lead times. X marks indicate the 95% confidence levels based on adjusted degrees of freedom. The light blue and yellow bars represent the skills based on the CESM-DP and the CESM-LE, respectively.

Further investigation reveals that the SPG SST is an important source of predictability, and the predictions based on the SPG SST alone demonstrate higher skills than those based on the MDR SST alone. In addition, the dependence of retrospective forecast skill on the ensemble size is explored. The prediction skill based on the Pearson correlation quickly increases when the ensemble size is increased from 1 to 5 and saturates when the ensemble size is around 20, similar to the dynamic prediction of seasonal TC activity, but the RMSE of ACE does not converge even for the ensemble size of 40.

The impacts of ocean initialization on prediction skill are examined by comparing the hybrid predictions based on the CESM-DP and CESM-LE experiments (Kay et al. 2015), with the latter serving as the uninitialized counterpart to the CESM-DP (Fig. 11). Initialization of ocean and sea-ice does not strongly affect TC frequency prediction, but significantly increases the prediction skill of ACE, landfalling hurricane frequency, hurricane and major hurricane days. Further analysis shows that the variability of the AMOC and the SPG SST are skillfully predicted in the CESM-DP but not in the CESM-LE. The key role of oceanic dynamics in driving the decadal variability of North Atlantic SST has been recognized by recent studies, and initializing the model with realistic subsurface ocean conditions in the CESM-DP contributes to the skillful predictions of the AMOC and the SPG SST. In contrast, the evolution of tropical SST is believed to be driven by radiative forcing associated with time-varying greenhouse gases and aerosols. The CESM-LE thus has skills in predicting the MDR SST even without the ocean initialization. The comparison also implies the role of external forcing in the variability of Atlantic basin-wide TC frequency.

Further analysis is conducted to evaluate how the SPG SST may affect the large-scale environmental conditions. It is shown that the SPG SST can modulate VWS and TPW over the tropical Atlantic independent of the MDR SST forcing, and it plays a role in modulating the strength of the Atlantic regional Hadley circulation. In addition to being affected by the local SST, the atmospheric circulation over the tropical Atlantic is also subject to remote SST forcing from the Pacific. Although the hybrid model does not use any SST index from the Pacific, the significant correlation between the observed SPG SST and PDO indices suggests that the remote influence from the Pacific is partly represented by the SPG SST in the hybrid model.

2.11 Skillful Seasonal Prediction of Eurasian Winter Blocking and Extreme Temperature Frequency (Miller and Wang 2019)

Atmospheric blocking is a major producer of extreme weather events that have profound socioeconomic impacts. However, few strides towards seasonal prediction of atmospheric blocking have been made. We developed a new statistical model for prediction of the winter seasonal blocking frequency over Eurasia one month in advance. The model employs the September SST, September Z70, and October sea ice coverage (SIC) as predictors. The correlation between the two timeseries is 0.81 and is above the 99% confidence interval based on the t-test and bootstrap test, suggesting that about 66% of the interannual variance of blocking frequency was captured by our prediction model (Fig. 12). The model also successfully captured some extreme years (e.g., 1984, 2005, 2011). Although this study is partly motivated by the skillful prediction of the NAO shown by some recent studies, the skillful prediction of blocking frequency cannot be completely attributed to the NAO, as the perfect knowledge of the winter NAO does not lead to a more skillful prediction of the seasonal blocking frequency (Fig. 12; r = 0.29), and the correlation between the winter NAO and Eurasian blocking frequency is -0.42.

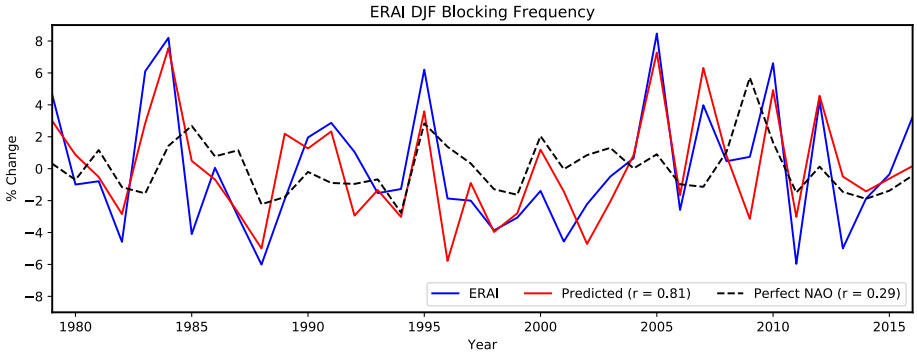

Fig. 12 Time series of observed and predicted mean Eurasian blocking frequency. Observed (blue), prediction from the multiple linear regression model (red), and prediction with the perfect knowledge of the winter NAO (dashed black) of the mean Eurasian blocking frequency change from winter 1979-2016.

Furthermore, we applied the same predictors used for blocking prediction to predict the seasonal occurrence of winter extreme hot and cold days. The Spearman Rank correlations between the observed and predicted cold and warm extreme day frequency. As in the prediction of blocking frequency, the leave-one-out cross-validation method was applied. Locally significant correlations between the predicted and observed cold extreme frequencies are located over Greenland and spans from the North Sea southeastward across central Asia towards Japan, and skillful and locally significant prediction of warm extremes exits over eastern Greenland and stretching across central Asia. Note that the regions of significant prediction of warm extremes shift northward as warm extremes are nearly co-located with the blocking high. Field significance was calculated using the False Discovery Rate (FDR). A majority of local test are field significant at the $\alpha_{FDR} = 0.10$ level (white contours) for both cold and warm extreme predictions, while localized regions of higher correlation values are significant at the $\alpha_{FDR} = 0.05$ level (green contours). Our prediction skill of the extreme temperatures is higher than the skill of some state-of-the-art-the-art dynamic models.

2.12 Hybrid Prediction of Weekly Tornado Activity out to Week 3: Utilizing Weather Regimes (Miller et al. 2020)

Severe convective storms produce strong winds (>25.9 m/s), large hail (25.4 mm), and/or tornadoes, and have the potential to induce significant socio-economic loss. In 2018 alone, tornadoes in the United States caused over 10 fatalities and greater than $600 million in combined property and crop damage (National Weather Service (NWS) U.S. Natural Hazard Statistics). Skillful extended-range forecasts would allow emergency management agencies to better prepare for proactive and reactive measures.

Although tornado activity is modulated by low-frequency climate modes, such as the ENSO, MJO, and Global Wind Oscillation (GWO), these low-frequency modes only explain limited variability of tornado activity. Enhanced tornado activity can still occur even when these low-frequency climate modes suggest an overall inactive time period. It is likely that synoptic-scale events strongly modulate the environmental conditions on the shorter time scales and induce tornado outbreaks even when the climate modes suggest otherwise. If predictability exists for the statistics

of such synoptic-scale events, effectively exploiting this source of predictability can help improve the S2S prediction of severe storm activity.

To investigate the synoptic-scale events that may contribute to enhanced tornado activity, we explore skillful tornado prediction on the weekly time scale by employing the concept of weather regimes (WRs). Five WRs are identified over North America using daily 500-hPa geopotential field for May, the peak season for tornado activity (Fig. 13). A persistent WR is defined as a WR lasting at least three days. Tornado outbreaks are found to be associated with persistent occurrence of WRs (Fig. 14), especially WR1 and WR4. For example, the tornado outbreaks during May 17-29, 2019 are associated with a persistent WR1. Additionally, the tornado outbreak in May 5-10, 2015 is associated with a persistent WR4. About 75% of the tornado days (≥1 tornado) are associated with a persistent WR (Fig. 14b) while 26% of the tornado days occur during a persistent WR1. Similarly, 75% of all outbreak days (≥10 tornadoes) occur during a persistent WR while 43% of all outbreak days occur during a persistent WR1 (Fig 14c).

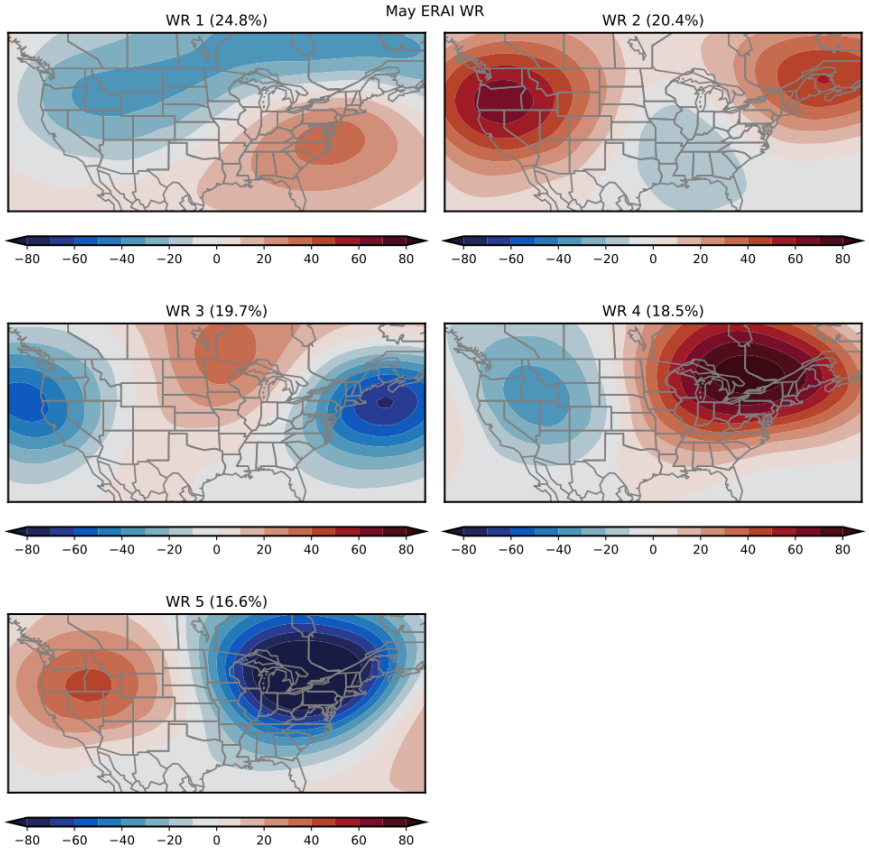

Fig. 13 The H500 patterns for five WRs over North America during May ordered from most frequent (WR1) to least frequent (WR5). The frequencies of occurrence are listed at the top of each sub-figure.

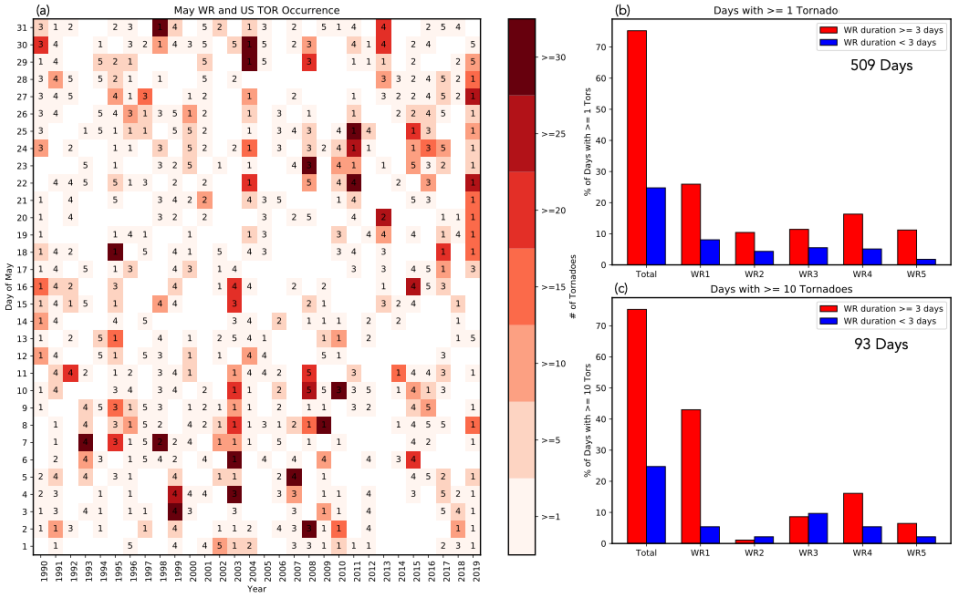

Fig. 14 (a) US tornado days (color shading indicates number of tornadoes per day) and WRs (numbers) during May 1990-2019. Non-tornado days are masked with white. Bar charts display the percentage of days with (b) ≥1 tornado and (c) ≥10 tornadoes for persisting (red) and non-persisting (blue) WRs.

The probability of tornado occurrence for each regime (regardless of duration) is also examined relative to climatology for different regions (not shown). The probability of occurrence of ≥5 tornadoes on a WR1 day for the US is >65%, or 13% above climatology. In brevity, tornado day occurrence is enhanced during WR1 in all regions except the NP, reduced during WR2 in all regions except the NE, enhanced during WR3 in the SP and NP, enhanced in all regions during WR4 except the NE and SE, and reduced during WR5 in each region (negligible change over SE). The modulation of WRs on the regional tornado activity can be explained by the changes in S900 and CAPE (not shown).

We developed a hybrid model to predict the weekly tornado activity, which is defined as the number of tornado days over a 7-day period. First, we perform K-means clustering on each ensemble member of ECMWF S2S prediction. The weekly WR frequency is calculated for each regime from days 1-7 to days 21-27 from individual ensemble members. Next, the weekly tornado activity is predicted using the ensemble member's WR frequency and the observed tornado frequency distributions of the training data set. The tornado predictions are carried out for each ensemble member, and the ensemble mean is used for the final tornado activity prediction. The prediction is evaluated against the observed weekly tornado day anomalies.

Figure 15a shows the HSS of the hybrid model in predicting the number of tornado days per week. Only the US, SP, and MW are shown for brevity. The HSSs are between 20-30% for shorter lead times and remain positive well into week 3, especially for the US and MW, implying that the empirical model adds knowledge relative to climatology. The same model can be used to predict the number of days with ≥5 tornadoes (Fig. 15b). The predictions are better than climatology well into week 3 and 4, with the MW showcasing the largest skill. However, the HSSs have large fluctuations due to the small sample size of the days with ≥5 tornadoes.

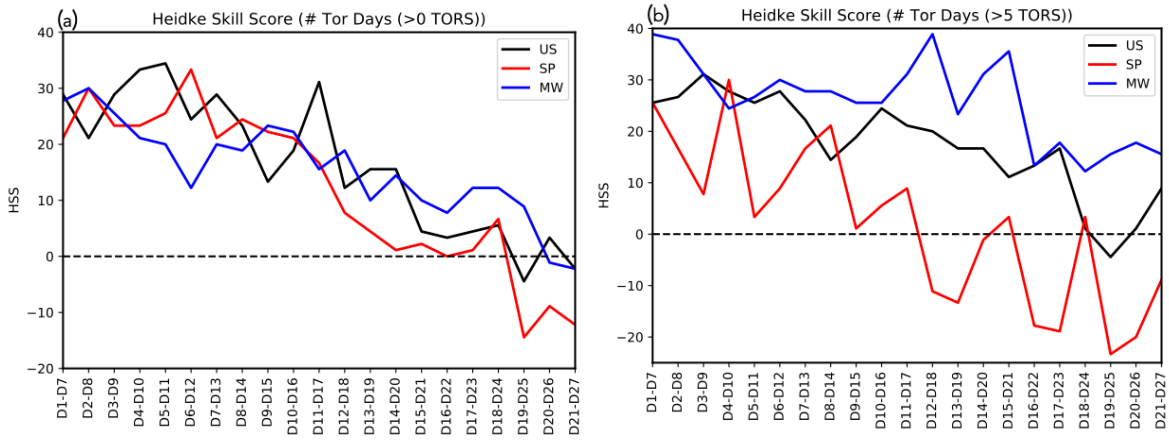

Fig. 15 HSS (%) for the hybrid prediction model predicting number of days per week with (a) >0 tornadoes and (b) >5 tornadoes for the United States (black), Southern Plains (red), and Midwest (blue).

2.13 Skillful Week 3-4 Prediction of United States Extreme Warm Days and SPI in Boreal Summer (Miller et al. 2020)

Despite the growing need of skillful prediction of extreme heat events at longer lead-times, especially in a warming climate, operational models produce far lower skill than desired past week-2 due to the intrinsic predictability limit of our atmosphere. Therefore, we investigated statistical techniques to produce skillful predictions of extreme warm days and precipitation at the week 3-4 lead times (Fig. 16). A North Pacific SST (NP SST) index and the second leading principle component of soil moisture are the two predictors which contribute to greater skill at weeks 3-4 over the Climate Forecast System, version 2 (CFSv2). Extreme NP SST index events are associated with a wave train that spans from the western Pacific Ocean to the eastern United States and induces a significant increase in blocking frequency, and therefore extreme warm days and negative SPI. Further analysis shows that blocking frequency at weeks 3 and 4 can be predicted skillfully using the NP SST index as a predictor. Summer blocking events are difficult to predict as patterns of variability, such as the NAO and ENSO, are weaker in Summer than in Winter. Extreme soil moisture events lead to significant persistence of dry soil-moisture, an increase in sensible heat flux, and an increase in blocking events that produce an increase in extreme warm days and low precipitation periods.

The results of this study highlight the importance of sea surface temperature and soil moisture in skillful long-range prediction of extreme heat events. It is important to reiterate that the predictors influence the occurrence of extreme heat events with a few weeks lag, and a model like the one used in this study should be used in conjunction with operational models as the operational forecast skill is much larger at week-1 and week-2. The MLR model here may serve as a bench mark for operational models at weeks 3 and 4, while aiding in mitigation of extreme heat events.

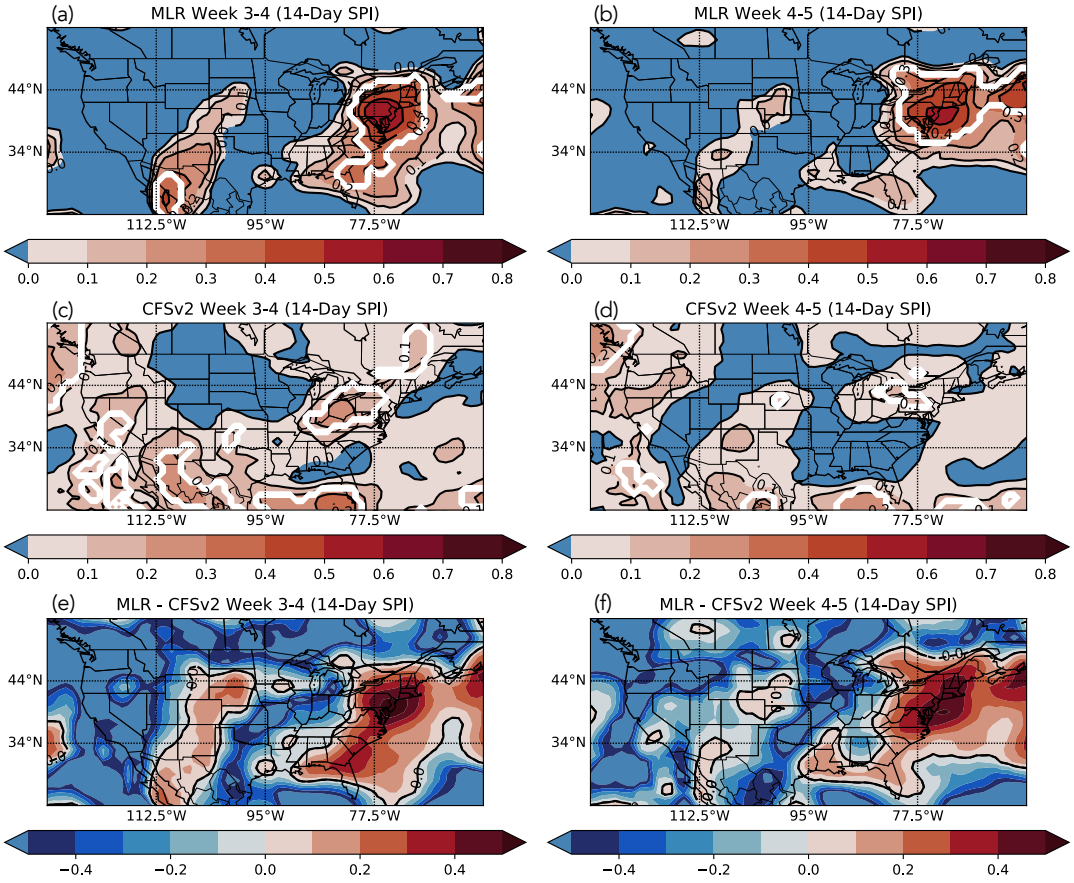

Fig. 16 Spearman rank correlation coefficient between the MLR predicted 14-day SPI and observations at (a) week 3-4 and (b) week 4-5. Spearman rank correlation coefficient between the CFSv2 predicted 14-day SPI and observations at (c) week 3-4 and (d) week 4-5. The difference in skill between the MLR and CFSv2 at (e) week 3-4 and (f) week 4-5. White contours indicate significant correlations at the $\alpha = 0.05$ *level using the varying degrees of freedom.*

3. Highlights of Accomplishments

- Thirteen papers were published, and two more are in preparation
- PhD graduate supported or partially supported: Gan Zhang, Doug Miller, Jay Chang
- More than twenty conference presentations by the PI and her students
- Diagnostics of TUTT, weather regimes, and blocking will be transitioned to a community model diagnostic package

4. Publications from the Project

Peer-reviewed publications

1. *Zhang, G., Z. Wang, M. Peng, and G. Magnusdottir, 2017: Characteristics and Impacts of Extratropical Rossby Wave Breaking during the Atlantic Hurricane Season, J. Clim., 30, 2363-2379.
2. *Hu, H., F. Dominguez, Z. Wang, D. A. Lavers, F. M. Ralph and G. Zhang, 2017: Linking Atmospheric River Hydrological Impacts on the U.S. West Coast to Rossby

Wave Breaking, J. Clim., 30, 3381-3399.
3. *Wang, Z., W. Li, M. S. Peng, X, Jiang, R. McTaggart-Cowan, and C. Davis, 2018: Predictive Skill and Predictability of North Atlantic Tropical Cyclogenesis in Different Synoptic Flow Regimes, J. Atmos. Sci., 75, 361-378.
4. *Zhang, G., and Z. Wang, 2018: North Atlantic Extratropical Rossby Wave Breaking during the Warm Season: Wave Life Cycle and Role of Diabatic Heating, Mon. Wea. Rev., 146, 695-712.
5. *Jiang, X., B. Xiang, M. Zhao, T. Li, S.-J. Lin, and Z. Wang, 2018: Predictability of Cyclogenesis in a Global High-Resolution Coupled Model System, J. Clim., 31, 6209–6227.
6. *Chang, C.-C., and Z. Wang, 2018: Relative Impacts of Local and Remote Forcing on Tropical Cyclone Activity in Numerical Model Simulations, Geophys. Res. Lett., 45. doi.org/10.1029 /2018GL078606.
7. *Li, W., Z. Wang, G. Zhang, M. Peng, S. Benjamin, and M. Zhao, 2018: Subseasonal Variability of Rossby Wave Breaking and Impacts on Tropical Cyclones during the North Atlantic Warm Season, J. Clim., J. Clim., 31, 9679–9695.
8. *Miller, D.E. and Z. Wang, 2019: Assessing Seasonal Predictability Sources and Windows of High Predictability in the Climate Forecast System, Version 2. J. Clim., 32,1307–1326.
9. *Zhang, G*., and Z. Wang, 2019: North Atlantic Rossby Wave Breaking during the Warm Season: Reconciliation of Tropical and Extratropical Impacts on Atlantic Hurricane Activity, J. Clim., 32, 3777-3801.
10. *Miller, D. E., and Z. Wang, Z., 2019: Skillful seasonal prediction of Eurasian winter blocking and extreme temperature frequency. Geophysical Research Letters, 46, 11,530–11,538. https://doi.org/ 10.1029/2019GL085035
11. *Chang, C. and Z. Wang, 2020: Multi-Year Hybrid Prediction of Atlantic Tropical Cyclone Activity and the Predictability Sources. J. Climate, 33, 2263–2279.
12. Miller, D.E.*, Z. Wang, Robert J. Trapp, and Daniel S. Harnos, 2020: Hybrid Prediction of Weekly Tornado Activity out to Week 3: Utilizing Weather Regimes. Geophys. Res. Lett. 47. https://doi.org/10.1029/2020GL087253.
13. Wang, Z., G. Zhang, T. Dunkerton, and F. Jin, 2020: Summertime Stationary Waves Integrate Tropical and Extratropical Impacts on Tropical Cyclone Activity, Proceedings, National Academy of Sciences, 202010547; DOI: 10.1073/pnas.2010547117.
14. Miller, D.E.*, Z. Wang, B. Li, Daniel S. Harnos, Trent Ford, 2020: Skillful Week 3-4 Prediction of United States Extreme Warm Days and SPI in Boreal Summer, to be submitted to Geophys. Res. Lett.
15. Miller, D.E.* and Z. Wang, 2020: Onset Mechanisms and Predictability of Boreal Winter Blocking, in preparation.

5. PI Contact Information

Zhuo Wang
Department of Atmospheric Sciences
University of Illinois at Urbana-Champaign
3056 Natural History Building, 1301 W Green Street
Urbana, IL 61801 Tel: (217) 244-4270